Development of the WAter-interface Permeation In Tritium-exposed materIals (Wapiti) tritium experiment and preliminary Eurofer97 results

F. Montupet-Leblond, Elodie Bernard, S. Feuillastre, S. Garcia-Argote, E.A. Hodille, M. Payet, C. Grisolia

Nuclear Materials and Energy 38 (2024) 101561

Contents lists available at ScienceDirect

Nuclear Materials and Energy

journal homepage: www.elsevier.com/locate/nme

Development of the WAter-interface Permeation In Tritium-exposed materIals (Wapiti) tritium experiment and preliminary Eurofer97 results

F. Montupet-Leblond [a,*], E. Bernard [a], S. Feuillastre [b], S. Garcia-Argote [b], E.A. Hodille [a], M. Payet [a], C. Grisolia [a]

[a] Institut de Recherche sur la Fusion par Confinement Magnétique, CEA Cadarache, 13115 St Paul lez Durance, France
[b] Service de Chimie Bioorganique et de Marquage, CEA Saclay, Université Paris-Saclay, 91191 Gif sur Yvette, France

ARTICLE INFO

Keywords:
Permeation
Trapping
Eurofer97
Tritium

ABSTRACT

The control of tritium inventory and permeation is crucial for the safe operation of fusion reactors. To measure these phenomena, a novel tritium experiment is introduced and used to measure tritium permeation through Eurofer97 at room temperature, with several possibilities for the downstream conditions: air or water and overhead air. A pre-loading condition was shown to be required for this experiment. This direct comparison revealed that tritium is preferentially found in the water phase and secondarily in the air phase.

1. Introduction

Controlling the tritium trapping and permeation in and through the walls of fusion reactors is a prerequisite for their safe operation [1]. To predict these phenomena, a precise understanding of the properties of fusion-relevant materials is required. A novel tritium permeation experiment called Wapiti (WAter-interface Permeation In Tritium-exposed materIals) is introduced in the present work, along with its experimental protocol. This experiment aims at measuring tritium permeation at room temperature with the possibility of adding water to the downstream medium.

The MHIMS model for diffusion and trapping of Eurofer97 introduced in [2] to replace the effective diffusivity model, which is not suitable for materials with multiple trapping sites, is then used to select the optimal conditions for the Wapiti Eurofer97 measurements. This analysis reveals that the high-energy trapping sites need to be filled for permeation to take place within a reasonable time frame. This filling of the trapping sites is performed by exposing the sample to tritium at 150 °C.

A first comparison of tritium permeation through Eurofer97 with either air or water and air as the downstream medium is then performed. This experimental analysis reveals that the measured permeation fluxes into the water are larger than the ones measured in air; furthermore, the presence of water decreases the amount of tritium found in the accompanying air phase. Further experiments are required to identify the underlying processes and separate surface effects from bulk ones.

2. State of the art

The transport parameters (diffusivity D, permeability Φ and solubility K) of hydrogen and deuterium in Eurofer97 have been measured by several teams using gas-driven permeation experiments and found to be in agreement [3–6]. The Arrhenius plot of diffusivity indicates that permeation is not purely interstitial. The deviation from the usual $D(T) = D_0 \exp \frac{-E_D}{k_B T}$ is attributed to the influence of trapping. The effective diffusivity model proposed by Oriani [7] is therefore used to model this hybrid behavior, as shown in Fig. 1.

This behavior calls for an additional investigation of the trapping behavior in this material, which can be performed through Thermal Desorption Spectrometry (TDS) experiments. The study detailed in [2] uses both this technique and simulations of permeation experiments performed with the MHIMS code [8] to yield a model that satisfyingly reproduces hydrogen permeation and deuterium desorption experiments. This model includes three trapping sites, two of which have rather high detrapping energies (1.27 eV and 1.65 eV). This model is limited in its validity by the experiments that were used to establish it; in particular, none of these experiments were performed with tritium, although this isotope is the relevant one for safety regards. Tritium experimental results are scarce, and direct comparisons between tritium and deuterium or hydrogen permeation experiments on RAFM steels are even scarcer; [9] finds a diffusivities ratio close to $\sqrt{3/2}$ for experiments conducted on F82H (a material also belonging to the RAFM family) at higher temperatures, but mentions a deviation from

* Corresponding author.
E-mail address: floriane.leblond@cea.fr (F. Montupet-Leblond).

https://doi.org/10.1016/j.nme.2023.101561
Received 4 August 2023; Received in revised form 27 November 2023; Accepted 28 November 2023
Available online 10 December 2023

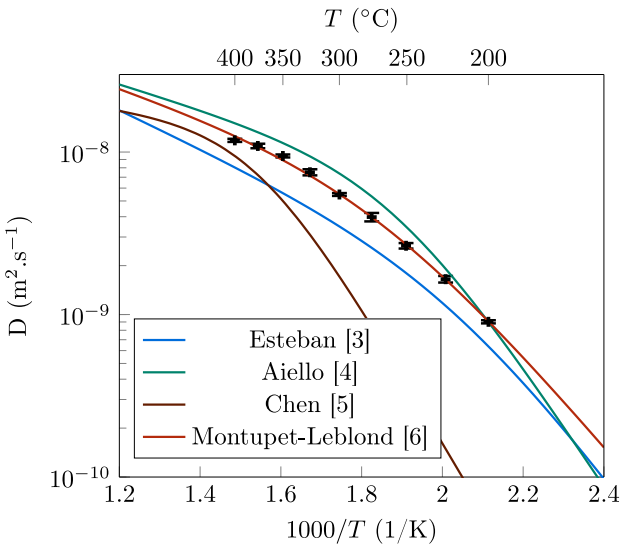

Fig. 1. Hydrogen diffusivity in Eurofer97, measured with gas-driven permeation experiments and modeled with effective diffusivity. Experimental data obtained with the Hypertomate experiment [6] are also displayed.

the classical square root of the masses ratio approach at lower temperatures, likely because of the influence of trapping. Few other tritium results are available, such as HT diffusivity in Eurofer97 [10]. Tungsten has been the focus of most of the tritium permeation studies [11,12]. Operating an experiment with tritium brings opportunities beyond what hydrogen and deuterium have to offer: desorption into water can be measured easily with Liquid Scintillation Counting (LSC) and the detection limit of tritium is considerably lower than that of deuterium or hydrogen due to its beta emission, which makes the detection of room-temperature permeation fluxes possible. The goal of the Wapiti experiment introduced in the present paper is therefore to explore these particular conditions: room-temperature permeation and permeation with the downstream medium containing water.

3. Experimental setup

The Wapiti experiment is a simplified version of the Hypertomate experiment introduced in [6], adapted to the tritium environment constraints and in particular to the limited available space in the glovebox. It consists of three independent and identical permeation cells that contain tritium upstream and either air or water and air in the downstream enclosure, as shown in Fig. 2. The upstream volumes have been minimized to around 2 ml each to mobilize the smallest possible amount of tritium for each experiment.

During an experiment, the three-way valves on top of each permeation cell are on bypass mode: the permeating tritium accumulates in the downstream enclosures. To perform a measurement, the valves are opened to sweep air into the cells. The permeated tritium that flows to the bubbler associated with the permeation cell, where tritium is accumulated. Each bubbler consists of four feeding bottles, with the first two accumulating HTO and the last two HT. The bubblers are located outside of the glovebox to lower their background noise and make sampling easier. For experiments including water in the downstream enclosure, the water is directly sampled and its activity is measured using LSC.

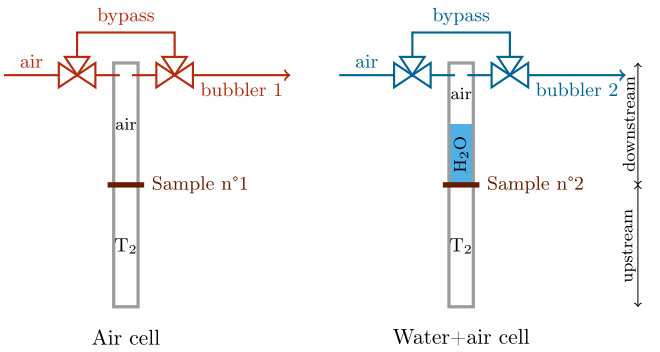

Fig. 2. Diagram of two side-by-side Wapiti permeation cells, one of them containing water downstream.

4. Experimental protocol

4.1. Tritium injection and reabsorption

The tritium injection is performed in a dedicated glovebox that contains the tritium source. Tritium is stored as uranium tritide: following the reaction $2U + 3T_2 \leftrightarrow 2UT_3$, gaseous tritium is released by heating up the uranium bed. Reciprocally, tritium is reabsorbed by lowering the temperature of the uranium bed. Fig. 3 shows a Wapiti permeation cell connected to the tritium loading rig. The tritium pressure is measured using piezo gauges P_1 and P_2. Valve V_C connects the device to a turbopumping unit, whose exhaust is sent to the laboratory chimney. Tritium releases are carefully monitored and avoided by reabsorbing on the uranium beds as much as reasonably possible.

The standard injection procedure consists of four steps (additional leak detections can be performed):

1. Permeation cell connection: using the VCR® fitting shown in Fig. 3, the Wapiti cell is connected to the tritium loading rig. Valves V_P, V_1, V_2 and V_3 are then opened to evacuate the residual pressure. After a few minutes of pumping, V_2 is closed and the pressure measured by P_1 is checked to remain constant. This step ensures that no major leak is present.
2. ^{3}He cleaning: a first desorption–reabsorption cycle is performed. If a residual pressure is measured once the uranium bed is back to room temperature, it is attributed to ^{3}He resulting from T decay and released to the chimney. The absence of tritium from this release is monitored at the chimney. This initial step ensures that the subsequent releases will only contain pure T_2.
3. T desorption: with all valves open except V_C, the uranium bed is heated up until the target tritium pressure is reached (between 50 mbar and 1 bar). Valve V_P is then closed and the tritium remaining between valves V_P and V_C is reabsorbed by cooling down the uranium bed. This method guarantees an optimized use of the exact amount of tritium required for the experiment.
4. Resting: following the desorptions of T_2 from the uranium bed, the background contamination of the glovebox increases. The permeation cell is left for several ventilation cycles inside the glovebox to decrease the contamination of the glovebox atmosphere.
5. Transfer: Once the glovebox contamination is back to acceptable levels, the permeation cell is cleared by the safety officer and transferred under their supervision to the dedicated Wapiti glovebox, where the measurements take place. By moving the permeation cells to a second glovebox that does not contain the tritium source, the background noise of the measurement is considerably lowered.

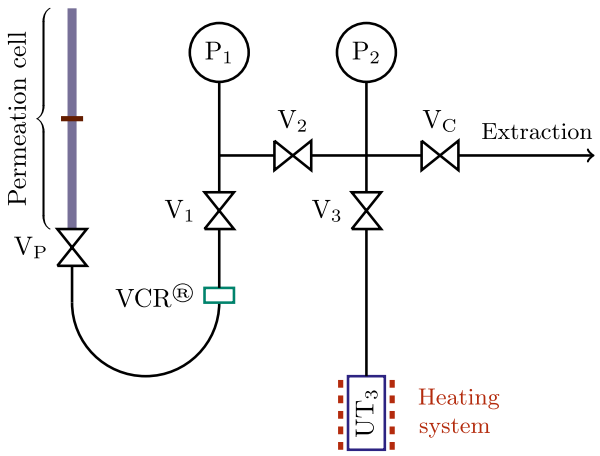

Fig. 3. Diagram showing a Wapiti permeation cell connected to the uranium tritide bed.

4.2. Permeation measurements

Once a permeation cell has been transferred to the dedicated measurement glovebox, it is connected to its associated bubbler. A diagram presenting the working principle of a tritium bubbler is shown in Fig. 4: the gas containing tritium flows through four bottles (B_1 to B_4) filled with micro-filtered water. In bottles B_1 and B_2, tritium in the HTO form is captured; HT remaining in the airflow is oxidized by the catalytic oven and captured in bottles B_3 and B_4. After the gas containing tritium has flowed through the bubbling system, the four bottles are simultaneously opened and water is sampled from each one of them. The volume of these samplings is typically around 1 mL. The four resulting samples are then analyzed with the lsc technique, which measures the tritium volumetric activity in tritiated water samples.

Because bubblers accumulate the activity over the course of the experiment, the experimental protocol is adapted to separate the background contributions from actual measurements. Each measurement of the air phase is done following three steps:

1. Background sampling of the four bottles in the bubbling system to obtain $A_n^{\text{background}}$, the background activity corresponding to the nth experimental point
2. Permeation cell sweep
3. Permeation sampling: the four bottles are sampled a second time, which yields $A_n^{\text{permeation}}$, the activity of the nth experimental point.

The cumulated activity corresponding to the nth sampling is subsequently evaluated as

$$A_n = A_{n-1} + A_n^{\text{permeation}} - A_n^{\text{background}} \quad (1)$$

In the case of a water–air cell (as shown in the right part of Fig. 2), the air is sampled first, after which the top part of the cell is opened to allow for direct sampling of 1 mL of water. This volume of water is immediately replaced by 1 mL of pure distilled water. The dilution created by this operation is taken into account in the processing of the data.

4.3. Measurement error evaluation

Typical gas-driven permeation experiments (such as Hypertomate introduced in [6]) have a high repeatability due to the cyclic nature of permeation measurements at higher temperatures. In the case of Wapiti, the experiment is not repeated in cycles due to the complexity of tritium injection, release and reabsorption combined with the slow permeation rate that makes experiments last for several weeks. As a preliminary estimation, the measurement error of Wapiti can be conservatively evaluated:

- The trapping efficiency of HT and HTO in the tritium bubbling systems leads to an error of ± 10% on tritium activity
- The sampling error caused by the re-sampling that is necessary to perform LSC measurements is also ± 10%
- The technical specifications of the scintillation counter report a 63% minimal efficiency for tritium, which means that the tritium contamination can be underestimated by around 35%.

Using Gaussian error propagation, we consider in the following that the measurement error of Wapiti is −14%/+38%. This conservative evaluation is expected to be replaced by a more precise one based on repeatability once more runs of the experiment will have been performed.

5. Preparation of the experimental protocol using the mhims model

5.1. MHIMS evaluation of the permeation timelag

The Wapiti experiment operates at room temperature: the permeation fluxes are expected to be orders of magnitude lower than the ones measured with high-temperature experiments such as Hypertomate [6], and similarly the time required for tritium to reach the downstream side of the sample (referred to as timelag in the following) is much longer.

Estimating the timelag is necessary to prepare the tritium experiments. Because the effective diffusivity model that conveniently evaluates the timelag as $\tau_L = \frac{e^2}{6 \cdot D_{\text{eff}}}$ is not suitable for Eurofer97 as shown in [2], more complex models are required.

The three-traps model for Eurofer97 in MHIMS can be used to estimate the timelag. The results need to be treated as qualitative only, as this model has only been validated against hydrogen and deuterium results obtained at higher temperatures.

Fig. 5 displays the result of a MHIMS simulation that uses the three-traps and kinetic surface model introduced in [2], with a loading pressure taken at 500 mbar of pure T_2. We can notice in this figure that after a full year, the permeation front has not reached the first 2 μm, although permeation samples are typically 500 μm thick. This simulation indicates that room-temperature tritium permeation in Eurofer97 cannot be measured within an acceptable time.

5.2. Loading protocol

The permeation cycles simulations performed in [2] have shown that the presence of irreversible trapping sites in Eurofer97 leads to a considerable increase in the first timelag, because of the extra time needed to fill these sites. However, because these sites remain full during subsequent permeation cycles, this effect only occurs on the first timelag.

The room-temperature permeation timelag can therefore be made shorter by filling the irreversible trapping sites. To that end, the following loading procedure is proposed to kick-start permeation in Eurofer97:

1. Tritium is injected in the upstream part of the cell, at the pressure picked for the permeation experiment.
2. The sample is heated up to 150 °C for 45 min using a heating cord wrapped around the cell. The temperature and duration of the loading step were set to fit the safety requirements of the glovebox.
3. The sample cools down relatively quickly (in a matter of minutes) thanks to the active ventilation of the glovebox.
4. Tritium is reabsorbed on the uranium bed.

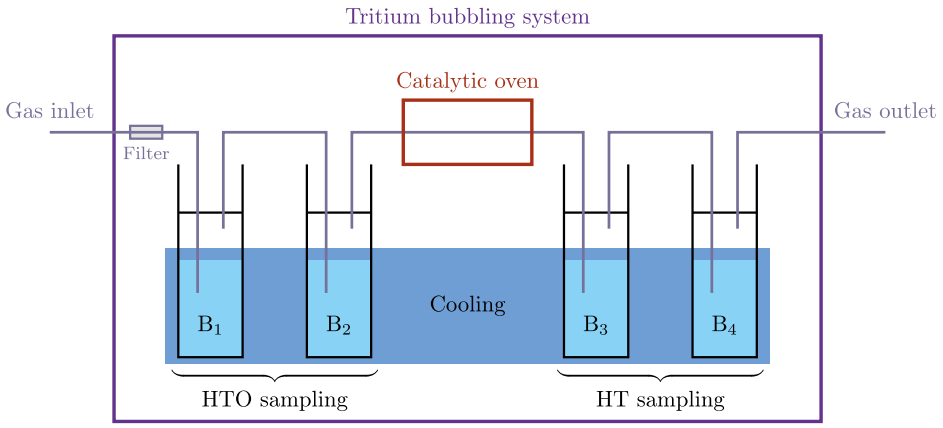

Fig. 4. Diagram presenting the main elements that constitute a tritium bubbling system. The gas flows through bottles 1 and 2, where HTO is captured; the remaining HT is then oxidized in the catalytic oven and captured in bottles 3 and 4.

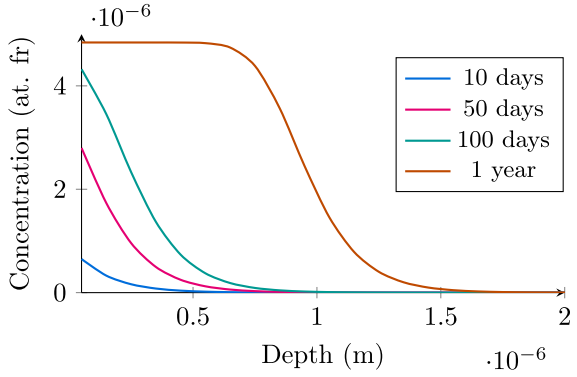

Fig. 5. MHIMS-simulated evolution of the tritium profile in Eurofer97 with the three-traps model.

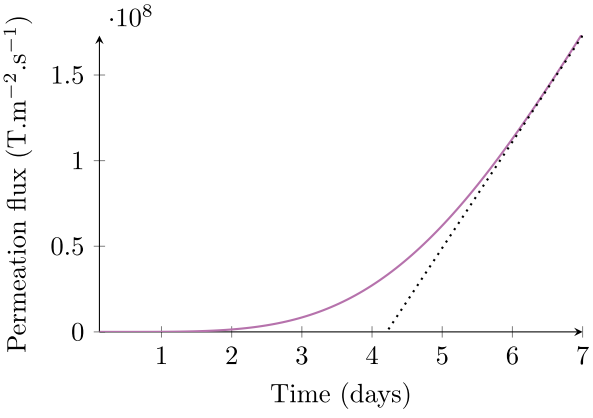

Fig. 6. MHIMS simulation of permeation through 420 µm of Eurofer97 with the first trap only, resulting in a timelag of around 4 days.

At the end of this loading procedure, the irreversible trapping sites in the sample are considered to be full and therefore not interfering with permeation any longer. The permeation timelag through the loaded sample can thus be estimated with MHIMS as done in Fig. 5 by removing the irreversible trapping sites from the model. The result of this simulation is shown in Fig. 6

The simulation results displayed in Fig. 6 indicate that the timelag through a 420 µm thick sample is reduced to around 4 days if the first trapping site is the only one considered. Fig. 7 shows a comparison between the permeation signal measured through a loaded sample and an unloaded one: tritium is only measured downstream of the loaded sample. This loading procedure is therefore applied to all subsequent Eurofer97 room-temperature tritium experiments.

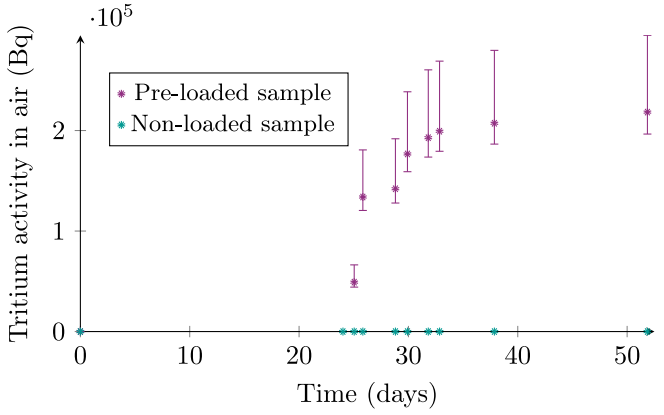

Fig. 7. Comparison of the cumulated activities measured through a pre-loaded and non-loaded sample, showing that the loading phase is required to measure a RT permeation signal through Eurofer97.

6. Comparison between tritium permeation into air and into water

6.1. Presentation of the results

For this comparison, the upstream conditions are the same for all three samples (250 mbar of pure tritium). All three cells underwent the loading procedure detailed in Section 5.2. In two of the cells, the downstream enclosure contains 4 mL of water and around 4 mL of air, while the third contains only air. Air is therefore sampled in all three cells, while water can only be sampled in cells 1 and 2. These experimental conditions are summarized in the diagram of Fig. 8.

The tritium activities measured in the downstream enclosures are shown in Fig. 9. The points where a permeation is established are connected by dashed lines and the corresponding permeation flux is indicated.

Fig. 9(a) compares the fluxes measured in the air phases of the three cells. Noticeably, the flux in the cell containing only air (1546 Bq day^{-1}) is much larger than the fluxes measured in the cells containing water and air (540 Bq day^{-1} and 247 Bq day^{-1}). This trend indicates that permeation takes place easier with a downstream phase of air only whereas the additional layer of water tends to slow down the permeation process into air.

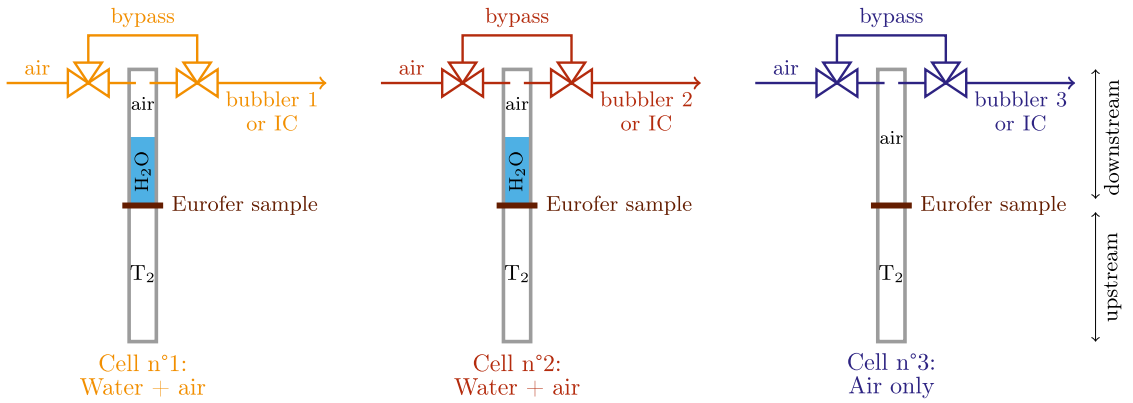

Fig. 8. Setup of the Wapiti experiment comparing Eurofer97 permeation with varying downstream conditions. The first two cells contain water and air downstream while the third one only has air downstream. All three samples have been loaded beforehand and the working pressure is 250 mbar of pure T_2.

Fig. 9(b) shows the fluxes measured in the water phases in cells 1 and 2. These fluxes are one order of magnitude higher than the ones measured in the air phases. This trend indicates that the accumulation of tritium resurfacing on the downstream surface is easier in water than in air.

From this comparison, we can extract the following trend for the permeation fluxes J_i:

$$J_{\text{water}} > J_{\text{air}} > J_{\text{air through water}}$$

6.2. Discussion and open questions

This preliminary comparison of permeation into water and into air raises questions that require additional experiments to be answered. First, we can notice that the fluxes measured in cell 1 are lower than those of cell 2, although the experimental conditions are supposedly identical for these two cells. This discrepancy could be caused by the growth of the oxide on the downstream surface that likely took place during the loading phase: as shown in [13], the presence of an oxide layer on Eurofer can reduce the permeation flux. This lead requires "post-mortem" analysis of the samples to be verified, which is difficult to perform on tritiated samples such as the ones of this study. The loading phase of the Wapiti experiment will therefore be repeated with hydrogen instead of tritium and the oxide layer will be characterized with XPS. Additionally, this tritium experiment will be performed again with a protective Pd coating to exclude surface effects from the analysis, as such a coating is expected to improve recombination [14].

The process through which tritium reaches the water phase also needs to be characterized. Once the permeating atoms reach the downstream surface exposed to water, they can either recombine with another surrounding tritium atom and form solute T_2 in the water phase or turn to HTO through isotopic exchange. In the specific case of Eurofer97, the interaction of water with the downstream surface also results in the formation of small rust particles: the rusting process is also likely participating in the contamination of the water. The propensity of Eurofer97 for rusting has been mentioned in [15], and [16] found the corrosion resistance of Eurofer97 and ODS-Eurofer to be lower than in standard stainless steels such as AISI 430. The present measurements do not discriminate between T_2, HTO and solid particles generated by the corrosion process. This separation will be performed in the future by centrifuging the water samplings. The tritium content of the resulting solid particles will then be analyzed with total dissolution [17]. Centrifuging is also expected to lower the amount of solute T_2: by comparing the activity levels before and after centrifuging, trends regarding the influence of the three possible processes will be extracted.

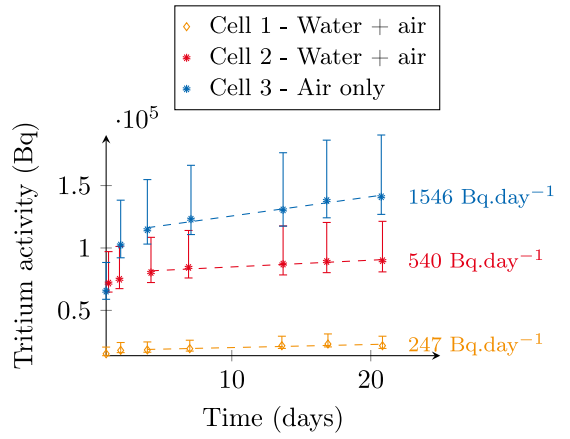

(a) Activity measured in the air phase of the three cells

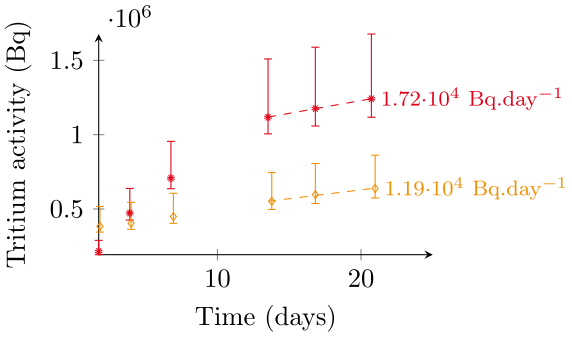

(b) Activity measured in the water phase of cells 1 and 2

Fig. 9. Permeation into air and into water.

7. Conclusion

Tritium permeation at room temperature through pre-loaded Eurofer97 samples was measured using the novel Wapiti experiment. In two of the cells, the downstream medium was water with an overhead air phase; the third cell contained only air downstream. The comparison between the fluxes measured downstream reveals that tritium is found primarily in the water phase and secondarily in the air phase. The presence of oxide layers on the downstream surfaces could explain the discrepancy witnessed between two similar permeation cells. Additional experiments were proposed to isolate surface effects and bulk ones, and to identify the contribution of isotopic exchange, T_2 dissolution and corrosion to the water contamination.

This work has been carried out within the framework of the EUROfusion Consortium, funded by the European Union via the Euratom Research and Training Programme (Grant Agreement No 101052200 – EUROfusion). Views and opinions expressed are however those of the author(s) only and do not necessarily reflect those of the European Union or the European Commission. Neither the European Union nor the European Commission can be held responsible for them.

CRediT authorship contribution statement

F. Montupet-Leblond: Conceptualization, Data curation, Formal analysis, Investigation, Methodology, Resources, Supervision, Writing – original draft, Writing – review & editing. **E. Bernard:** Data curation, Supervision. **S. Feuillastre:** Methodology, Resources. **S. Garcia-Argote:** Methodology, Resources. **E.A. Hodille:** Formal analysis. **M. Payet:** Data curation, Formal analysis, Investigation, Methodology. **C. Grisolia:** Funding acquisition, Project administration, Supervision.

Declaration of competing interest

The authors declare that they have no known competing financial interests or personal relationships that could have appeared to influence the work reported in this paper.

Data availability

Data will be made available on request.

References

[1] D. Perrault, Nuclear Fusion Reactors - Safety and Radiation Protection Considerations for Demonstration Reactors That Follow the ITER Facility, Institut de Radioprotection et de Sûreté Nucléaire, 2017.
[2] F. Montupet-Leblond, E.A. Hodille, M. Payet, R. Delaporte-Mathurin, E. Bernard, Y. Charles, J. Mougenot, S. Vartanian, C. Grisolia, Influence of traps reversibility on hydrogen permeation and retention in Eurofer97, Nucl. Fusion (2022).
[3] G. Esteban, A. Peña, I. Urra, F. Legarda, B. Riccardi, Hydrogen transport and trapping in Eurofer97, J. Nucl. Mater. 367–370 (2007) 473–477.
[4] A. Aiello, I. Ricapito, G. Benamati, R. Valentini, Hydrogen isotopes permeability in Eurofer97 martensitic steel, Fusion Sci. Technol. 41 (2002) 872–876.
[5] Z. Chen, X. Hu, M. Ye, B.D. Wirth, Deuterium transport and retention properties of representative fusion blanket structural materials, J. Nucl. Mater. 549 (2021) 152904.
[6] F. Montupet-Leblond, L. Corso, M. Payet, R. Delaporte-Mathurin, E. Bernard, Y. Charles, J. Mougenot, S. Vartanian, E. Hodille, C. Grisolia, Permeation and trapping of hydrogen in Eurofer97, Nucl. Mater. Energy 29 (2021) 101062.
[7] R. Oriani, The diffusion and trapping of hydrogen in steel, Acta Metall. 18 (1970) 147–157.
[8] E. Hodille, A. Založnik, S. Markelj, T. Schwarz-Selinger, C. Becquart, R. Bisson, C. Grisolia, Simulations of atomic deuterium exposure in self-damaged tungsten, Nucl. Fusion 57 (5) (2017) 056002.
[9] Y.N. Dolinsky, Y.N. Zouev, I. Lyasota, I. Saprykin, V. Sagaradze, Permeation of deuterium and tritium through the martensitic steel F82H, J. Nucl. Mater. 307 (2002) 1484–1487.
[10] A. Fedorov, S. Van Til, A. Magielsen, M. Stijkel, Tritium permeation and desorption in reduced activation martensitic steels studied in EXOTIC-9/1 irradiation experiment, J. Nucl. Mater. 442 (1–3) (2013) S723–S725.
[11] M. Shimada, R. Pawelko, Tritium permeability in polycrystalline tungsten, Fusion Eng. Des. 146 (2019) 1988–1992.
[12] H. Nakamura, T. Hayashi, T. Kakuta, T. Suzuki, M. Nishi, Tritium permeation behavior implanted into pure tungsten and its isotope effect, J. Nucl. Mater. 297 (3) (2001) 285–291.
[13] A. Houben, J. Engels, M. Rasiński, C. Linsmeier, Comparison of the hydrogen permeation through fusion relevant steels and the influence of oxidized and rough surfaces, Nucl. Mater. Energy 19 (2019) 55–58.
[14] E. Fromm, Effect of oxide layers on the absorption kinetics of hydrogen by metals at room temperature, Z. Phys. Chem. 147 (1–2) (1986) 61–75.
[15] M. Rieth, M. Dürrschnabel, S. Bonk, S. Antusch, G. Pintsuk, G. Aiello, J. Henry, Y. De Carlan, B.-E. Ghidersa, H. Neuberger, et al., Fabrication routes for advanced first wall design alternatives, Nucl. Fusion 61 (11) (2021) 116067.
[16] M. Terada, A.J. de Oliveira Zimmermann, H.R.Z. Sandim, I. Costa, A.F. Padilha, Corrosion behavior of Eurofer97 and ODS-Eurofer alloys compared to traditional stainless steels, J. Appl. Electrochem. 41 (2011) 951–959.
[17] S. Peillon, G. Dougniaux, M. Payet, E. Bernard, G. Pieters, S. Feuillastre, S. Garcia-Argote, F. Gensdarmes, C. Arnas, F. Miserque, et al., Dust sampling in WEST and tritium retention in tokamak-relevant tungsten particles, Nucl. Mater. Energy 24 (2020) 100781.